Determination of the energy-dependent conduction band mass in SiO$_2$

R. Ludeke[a)] and E. Cartier
IBM T.J. Watson Research Center, P.O. Box 218, Yorktown Heights, New York 10598

Andreas Schenk
*Integrated Systems Laboratory, Swiss Federal Institute of Technology, Gloriastrasse 35,
CH-8092 Zürich, Switzerland*

The energy dependence of the conduction band mass in amorphous SiO$_2$ was deduced from quantum interference oscillations in the ballistic electron emission microscope current, and separately from Monte Carlo simulations of the electron mean free paths obtained by internal photoemission. The results imply a strong nonparabolicity of the conduction band of SiO$_2$. © *1999 American Institute of Physics.* [S0003-6951(99)00836-0]

The effective mass m_{ox} of conduction band electrons in SiO$_2$ is a fundamental parameter that enters into the description of virtually every aspect of hot electron transport in metal–oxide–semiconductor (MOS) based structures and devices.[1] The mass directly affects the electron-phonon coupling strengths that determine scattering rates in SiO$_2$, which in turn determine the thermalization of hot electrons,[2] charge trapping/detrapping phenomena,[3] and ultimately device degradation processes.[4] Nevertheless m_{ox} has not been measured unequivocally and considerable disparities have been reported.[5–7] The suggestion that m_{ox} is dispersive, i.e., $m_{ox} = m_{ox}(E)$, where E is the kinetic energy of the conduction band electron, was already made by Maserjian[5] and subsequently addressed by others.[1,8] A dispersive m_{ox} is also evident from band structure calculations for all polytypes of quartz.[9–11] However, a direct measurement has not been previously reported. We present in this letter two independent determinations of $m_{ox}(E)$ that are in qualitative agreement over a 0–3 eV kinetic energy (KE) range. Both rely on theoretical modeling with $m_{ox}(E)$ adjusted to fit experimental data. One method is based on quantum interference (QI) oscillations of electrons injected into a MOS structure with the tip of scanning tunneling microscope (STM), a technique called ballistic electron emission microscopy (BEEM).[7,8] The second determination is based on Monte Carlo (MC) simulations of the energy dependent attenuation lengths of the electrons obtained from internal photoemission experiments.[12]

The MOS structures were prepared in ultrahigh vacuum by evaporating 1.8–4 nm metal layers (W or Pd) through a shadow mask and onto oxides that were thermally grown *ex situ* on *p*-type Si(100). In BEEM the STM is biased at V_T relative to the metal film, which imparts the electrons with a KE of eV_T relative to Fermi level E_F of the metal. The electrons traverse the metal ballistically and may enter the conduction band of the SiO$_2$ if $eV_T > \Phi_B$, the barrier height between E_F and the SiO$_2$ conduction band edge. Electrons that reach the Si substrate are detected as an emerging ''collector'' current I_c. A bias V_b applied across the oxide can be adjusted to achieve flat band conditions, a preference that minimizes variations in KE as the electron traverses the oxide. In the spectroscopy mode the scanning of the STM tip is stopped temporarily and I_c is measured as a function of V_T. I_c may exhibit an oscillatory modulation arising from interference effects of the electron wave function in the oxide conduction band,[7,8] akin to those observed in Fowler–Nordheim (FN) experiments.[5,6,13–17] In the simplest model of a rectangular potential barrier, maxima in the transmission coefficient $\tau(E)$ are found at $(E - \Phi_B)^{1/2} = n\pi\hbar/d(2m)^{1/2}, n = 1,2,3...$.[18]

In the internal photoemission experiments electrons from a Pt substrate were excited with monochromatic light of energy $\hbar\omega$ and injected into the conduction band of 1–5 nm SiO$_2$ layers. A fraction of the electrons traverse the oxide and are emitted into the adjacent vacuum, where the thickness dependent energy distributions were measured as a function of $\hbar\omega$.[12,19] The energy distributions provide a quasidynamic picture of the thermalization as the electrons cross the oxide under zero field conditions. An exponential decay with increasing layer thickness d was observed:[19] $I(E,d) = I_0 \exp[d/L_a(E)]$, with $L_a(E)$, the attenuation length, representing a measure for the phonon scattering rates at energy E. The solid data points in Fig. 1 represent the values of $L_a(E)$ thus obtained over a 1–3.2 eV interval and are consistent with energy averaged values obtained from quantum interference[14] and internal photoemission experiments.[20]

We used a Monte Carlo solution of the Boltzmann transport equation in order to relate quantitatively the measured $L_a(E)$ to the scattering processes in SiO$_2$. We simulate the evolution of the electron distribution for various oxide thicknesses and extract $L_a(E)$ in exactly the same manner as for the experimental data. This procedure removes any ambiguity arising from different possible methods in defining $L_a(E)$. The unknown physical quantities such as the electron phonon coupling constants and/or the effective mass m_{ox} were then obtained in an iterative manner until an accurate match to the measured $L_a(E)$ was obtained. The MC routines and methods of calculating the electron-phonon scattering rates were those of Fischetti *et al.*[2,21] Electron scattering with LO, TO, and acoustic phonons were considered, with boundary conditions appropriate to the geometry.[22] Screening effects arising from the metal electrons were neglected.

[a)]Electronic mail: ludeke@watson.ibm.com
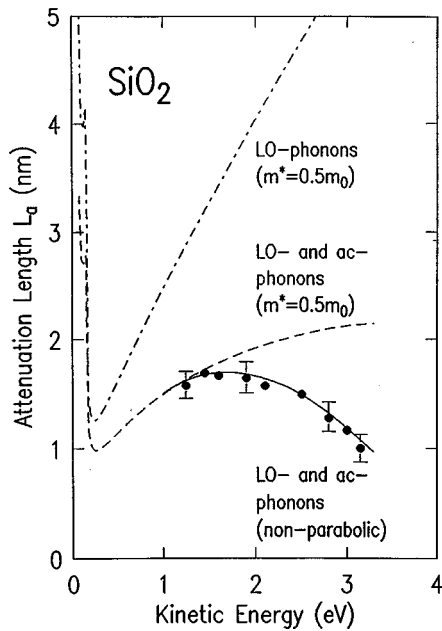
FIG. 1. Simulated (lines) and measured (dots) electron attenuation lengths in SiO_2 as a function of the electron kinetic energy. Dash-dotted line considers LO phonons only with $m_{ox} = 0.5 m_0$, dashed line includes both LO and acoustic phonon scattering with $m_{ox} = 0.5 m_0$, and solid line include in addition a dispersive m_{ox}.

FIG. 2. (a) BEEM spectrum I_c vs V_T for 1.8 nm W/3.0 nm SiO_2/p-Si(100) MOS structure (dotted curve), with I_c^0 shown by a dashed line. (b) experimental transmission coefficient, $\tau(E) \equiv I_c/I_c^0$ (dotted curve), compared to $\tau(E)$ calculated with a dispersive mass (solid curve). Vertical arrows mark QI maxima for $\tau(E)$ calculated with a fixed mass $m_{ox} = 0.42 m_0$. The threshold is at 3.77 V.

We initially assumed a parabolic conduction band described by $m_{ox} = 0.5 m_0$ and considered only electron scattering with LO phonon modes of 63 and 153 meV. The resulting $L_a(E)$, shown by dash-dotted line in Fig. 1, shows a sharp dip near 0.2 eV followed by a linear rise consistent with the coulombic nature of the electron interaction with LO phonons. The poor fit at higher energies is improved by including acoustic phonon scattering (dashed curve), with agreement to the experimental $L_a(E)$ at 1.5 eV premised on the choice of 6 eV for the acoustic phonon deformation potential. The subsequent deviations from the experimental data could not be reduced by the inclusion of TO mode scattering, nor by changing the nondispersive value of m_{ox} over a range from 0.3 to 0.7 m_0. Agreement could only be obtained by assuming an energy dependent $m_{ox}(E)$, with the resulting improved fit shown by the solid line in Fig. 1. Only LO and acoustic phonon scattering was included, and an electron velocity $v(E) = [2E/m_{ox}(E)]^{1/2}$ was assumed. The resulting $m_{ox}(E)$ will be discussed following the determination of m_{ox} from QI in BEEM.

A BEEM spectrum for a MOS structure with a 3 nm oxide is shown as a dotted curve in Fig. 2(a). An oscillatory structure is clearly observable. A bias $V_b = 0.3$ V (substrate positive) was applied across the oxide to assure flat band conditions.[23] All spectra were measured on areas of the sample not previously subjected to electron injection into the oxide (i.e., $V_T < |-3.77|$). Such prior exposures, particularly for $V_T > 6$ V, can generate positive oxide charge whose random distribution alters and even suppresses the QI structure.[7,24] The energy of the QI maxima are accurately determined by assuming that I_c is the product of the transmission coefficient $\tau(E)$ and an unmodulated component I_c^0: $I_c(E) = \tau(E) I_c^0(E)$. I_c^0 can be approximated by a simple power law curve tangential to the maxima in the BEEM spectrum, as shown by the dashed curve in Fig. 2(a). $\tau(E)$ is

then obtained by dividing I_c by I_c^0, with the results shown by the dotted curve in Fig. 2(b). This curve represents approximately the ''experimental'' $\tau(E)$, from which the positions of the QI maxima are readily obtained.

We will next outline the calculation of $\tau(E)$ and the procedure to match the maxima with those of the experimental $\tau(E)$. Details of the numerical solution of the one-dimensional (1D) Schrödinger equation can be found elsewhere.[7,25] Briefly, the barrier includes image force corrections arising from both metal-SiO_2 and SiO_2-Si interfaces, and is represented by a multistep potential approximation,[26] with continuity of ψ and $(1/m_{ox})(d\psi/dx)$ at each step boundary. Electron effective masses of m_0 and $0.19 m_0$ were assumed for the metal and Si conduction band electrons, respectively. Density of states mismatches across the interfaces were ignored. The results of calculating $\tau(E)$ with a constant mass, represented in Fig. 2(b) solely by arrows marking the maxima, shows agreement with experiment only for the first two maxima, to which the solution was intentionally fitted by setting $m_{ox} = 0.42 m_0$. Consequently, the mass was adjusted so that the first maximum agreed with the experimental one, thereby yielding $m_{ox}(E_1)$. Then m_{ox} was increased until agreement was reached for the second maximum, giving $m_{ox}(E_2)$. This procedure was continued for all subsequent maxima, yielding $m_{ox}(E_i)$ at peak energies E_i. Thus $m_{ox}(E_i)$ defines an absolute value of the mass and its dispersion at the discreet energies E_i. The resulting $\tau(E)$ is shown by the solid curve in Fig. 2(b). The values of $m_{ox}(E_i)$ are then used to obtain the dispersion curve represented by the dotted line in Fig. 3. Nearly coincident with this curve lies the solid line through data points that represent $m_{ox}(E_i)$ calculated for E_i values averaged from several spectra. Here we have subtracted the threshold energies to show the dispersions as a function of the KE of the conduction band electrons in SiO_2. The dashed curve is the mass dispersion of the averaged maxima with the assumption that the oxide thickness d is 2.9 nm. An uncertainty
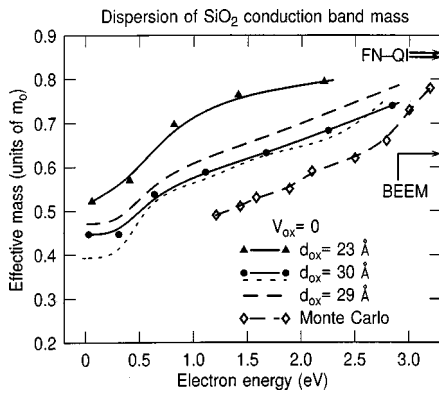
FIG. 3. Conduction band mass dispersions $m_{ox}(E)$ for SiO_2 determined from QI oscillations in BEEM spectra (top four curves), compared to dispersion derived from Monte Carlo simulations of experimentally determined electron mean free paths (lowest dash-dotted curve).

in d represents the most influential source for error in m_{ox}; estimated uncertainties in V_{ox} and Φ_B have a substantially smaller effect.[7]

The mass dispersion obtained from the MC simulations of the attenuation lengths in SiO_2 is shown by the open symbols in Fig. 3. Although the discrepancy with the BEEM-determined dispersion is substantial, the changes in mass over comparable energy intervals are quite close. Agreement cannot be expected since the ''reference'' mass for the MC calculations at 1.5 eV was assumed to be 0.5 m_0. No attempts were made to improve the agreement by increasing the mass in the MC calculations. Neither do we believe that the BEEM results overestimate the mass, as otherwise the band edge value ($E=0$) would correspond to an uncharacteristically low value of $<0.4\ m_0$.

We have also determined the dispersion for a 2.3 nm SiO_2 oxide, which was thermally grown on p-Si(100) and covered with 4 nm Pd metal layer.[25] The dispersion observed for this sample is shown by the topmost curve in Fig. 3. Its upward displacement relative to the 3 nm oxide cannot be accounted for by uncertainties in the parameters, particularly in their thickness. The latter were measured both by ellipsometer and by capacitance methods, with an uncertainty in relative thickness of less than 0.1 nm. Estimates of the absolute thickness are within ± 0.1 nm. Consequently, we must attribute the difference in the dispersions to thickness related phenomena, such as an onset of band structure changes.[27] The overall increase in $m_{ox}(E)$ for the thinner oxide is consistent with a narrowing of the bands due to the decreasing dimensionality.[28]

The range of the dispersions in all three cases, which are comparable in magnitude, implies considerable nonparabolicity in the conduction bands of SiO_2. The reduced dispersion at low KE, particularly for the 3 nm oxide, indicates an initial constancy of $m_{ox}(E)$ that implies a parabolic band behavior near the bottom of the conduction band. The value here of 0.44 m_0 is close to the best estimates of the tunnel mass $m_t=0.42\ m_0$ near the top of the gap,[5,29] and is consistent with the smooth transition between a Franz-type band dispersion in the gap and the bottom of the conduction band.[5]

Marked on the right ordinate of Fig. 3 near $m_{ox}=0.85$ m_0 are values obtained previously from QI in (FN)-injection experiments.[5,6] Their magnitude is considerably larger than the 0.63 m_0 value obtained recently by BEEM for a 2.8 nm oxide,[7] which was deduced from a single mass fit to data inferior to the results reported here. Nevertheless, its value agrees well with the energy-averaged dispersive mass for the 3 nm layer. The origin of the discrepancies with FN results are readily attributed to the greater sensitivity of m_{ox} to uncertainties in the FN parameters. Although m_{ox} depends inversely on d^2 in the QI criteria for both BEEM and FN experiments, its dependence on Φ_B is linear for BEEM[18] but cubic for FN,[6] which leads to serious errors in m_{ox} if Φ_B is not accurately known. Since for the high fields ($\sim 10^7$ V/cm) typical of FN injection Φ_B is quite sensitive to image force effects,[30] which were neglected in the FN experiments, substantial reductions in m_{ox} can be expected by their inclusion.[31]

[1] M. V. Fischetti, S. E. Laux, and E. Crabbé, J. Appl. Phys. **78**, 1058 (1995), and references therein.

[2] M. V. Fischetti, D. J. DiMaria, S. D. Brorson, T. N. Theis, and J. R. Kirtley, Phys. Rev. B **31**, 8124 (1985).

[3] D. J. DiMaria, E. Cartier, and D. A. Buchanan, J. Appl. Phys. **80**, 304 (1996).

[4] E. Cartier, Microelectron. Reliab. **38**, 201 (1998).

[5] J. Maserjian, J. Vac. Sci. Technol. **11**, 996 (1974).

[6] S. Zafar, K. Conrad, Q. Liu, E. A. Irene, G. Hames, R. Kuehn, and J. J. Wortman, Appl. Phys. Lett. **67**, 1031 (1995).

[7] H. J. Wen, R. Ludeke, and A. Schenk, J. Vac. Sci. Technol. B **16**, 2296 (1998).

[8] B. Kaczer, H.-J. Im, and J. P. Pelz, J. Vac. Sci. Technol. B **16**, 2302 (1998).

[9] P. M. Schneider and W. B. Fowler, Phys. Rev. B **18**, 7122 (1978).

[10] J. R. Chelikowsky and M. Schlüter, Phys. Rev. B **15**, 4020 (1977).

[11] Y.-N. Xu and W. Y. Ching, Phys. Rev. B **44**, 11048 (1991).

[12] J. Bernasconi, E. Cartier, and P. Pfluger, Phys. Rev. B **38**, 12567 (1988).

[13] J. Maserjian and G. P. Petersson, Appl. Phys. Lett. **25**, 50 (1974).

[14] M. V. Fischetti, D. J. DiMaria, L. Dori, J. Batey, E. Tierney, and J. Stasiak, Phys. Rev. B **35**, 4044 (1987).

[15] J. C. Poler, K. K. McKay, and E. A. Irene, J. Vac. Sci. Technol. B **12**, 88 (1994).

[16] S. Zafar, Q. Liu, and E. A. Irene, J. Vac. Sci. Technol. B **13**, 47 (1995).

[17] H. S. Momose, M. Ono, T. Yoshitomi, T. Ohguru, S. Nakamura, M. Saito, and H. Iwai, IEEE Trans. Electron Devices **45**, 1233 (1996).

[18] K. H. Gundlach, Solid State Electron. **9**, 949 (1966).

[19] E. Cartier and P. Pfluger, Phys. Scr. **23**, 235 (1988).

[20] R. Poirier and J. Olivier, Appl. Phys. Lett. **21**, 334 (1972).

[21] D. J. DiMaria and M. V. Fischetti, J. Appl. Phys. **64**, 4683 (1988).

[22] E. Cartier and F. R. McFeely, Phys. Rev. B **44**, 10689 (1991).

[23] D. A. Buchanan, F. R. Mc Feely, and J. J. Yurkas, Appl. Phys. Lett. **73**, 1676 (1998).

[24] H. J. Wen and R. Ludeke, J. Vac. Sci. Technol. A **16**, 1735 (1998).

[25] R. Ludeke and A. Schenk, J. Vac. Sci. Technol. B (to be published).

[26] Y. Ando and T. Itoh, J. Appl. Phys. **61**, 1497 (1987).

[27] The mass is inversely proportional to the 2nd derivative of the band dispersion $E(k)$ and therefore sensitive to band distortions and changes.

[28] F. Bassani and G. Pastori Parravicini, *Electronic States and Optical Transitions in Solids* (Pergamon, 1975).

[29] A. Schenk and G. Heiser, J. Appl. Phys. **81**, 7900 (1997).

[30] H. J. Wen, R. Ludeke, D. M. Newns, S. H. Lo, and E. Cartier, Appl. Surf. Sci. **123/124**, 418 (1998).

[31] See Eq. (2) of Ref. 6. Differentiating and solving for typical experimental parameters one obtains $\Delta m_{ox} \approx 5 m_{ox} \Delta \Phi_B / \Phi_B$. An estimate of the image force correction (not lowering) to the trapezoidal barrier for these values is $\Delta \Phi_B / \Phi_B = -qF/16\pi\epsilon\Phi_B^2 \sim 0.052$, where F is the oxide field and ϵ the permittivity. This results in a 26% lowering of m_{ox}.